This is the accepted manuscript (postprint) of the following article:
A. Yazdani, E. Salahinejad, *Evolution of reinforcement distribution in Al–B_4C composites during accumulative roll bonding*, Materials & Design, 32 (2011) 3137-3142.
https://doi.org/10.1016/j.matdes.2011.02.063

Evolution of reinforcement distribution in Al–B_4C composites during accumulative roll bonding

Ali Yazdani, E. Salahinejad*

Department of Materials Science and Engineering, School of Engineering, Shiraz University, Zand Blvd., 7134851154 Shiraz, Iran

* Corresponding Author: E-mail addresses: erfan.salahinejad@gmail.com

Abstract

The distribution of reinforcement particles in the matrix of a composite is one of the most important microstructural features affecting properties. In this study, nanostructured Al–B_4C composite sheets were processed by accumulative roll bonding (ARB), and the effect of the number of ARB cycles on the distribution of the B_4C particles in the Al matrix was evaluated. From optical microscopic studies accompanied by the radial distribution function analysis, it was realized that the microstructure uniformity is improved by increasing the number of ARB cycles. It was in good agreement with bulk hardness measurements in which the standard deviation of the hardness values was decreased by progression of the ARB process. In addition, the X-ray diffraction peak profile analysis revealed that the area weighted mean crystallite size of the Al matrix decreases to the nanometric scale (114 nm) after seven ARB cycles.

Keywords: Metal matrix composites; Nanomaterials; Microstructure

This is the accepted manuscript (postprint) of the following article:
A. Yazdani, E. Salahinejad, *Evolution of reinforcement distribution in Al–B_4C composites during accumulative roll bonding*, Materials & Design, 32 (2011) 3137-3142.
https://doi.org/10.1016/j.matdes.2011.02.063

1. Introduction

The development of metal matrix composites (MMCs) is of growing interest to scientific and industrial communities, due to their attractive physical and mechanical properties. Particularly, particulate reinforced aluminum MMCs have attracted considerable attention, because of lightweight, high strength, high specific modulus, low coefficient of thermal expansion and good wear resistance [1,2]. SiC, Al_2O_3, TiC and B_4C are common ceramic reinforcements in Al MMCs. Boron carbide (B_4C), which is a light ceramic, presents high mechanical properties, chemical resistance as well as neutron absorbing [3–6]. Applications of Al–B_4C composites include its use as a structural neutron absorber, armour plate materials, and as a substrate material for computer hard disks [7,8].

To meet the optimum properties of a composite, especially the best combination of high strength and good ductility, fine reinforcements and a relatively large particle volume fraction are required. Nonetheless, taking advantage of both of these requirements is a challenge, because MMCs with small particulates usually exhibit a very inhomogeneous particle distribution, degrading their ductility and formability [9–13]. A strong relationship between the local particle volume fraction and damage formation exists, where the damage formation is concentrated in particle clusters. In particle-reinforced MMCs with a clustered distribution, there is an accelerated development of damage during deformation. The stress distribution within a particle-reinforced composite subjected to external loading is non-uniform [11]. In the vicinity of a cluster, high stresses and stress triaxialities much higher than the remote stress applied to the composite are locally generated, leading to the acceleration of fracture initiation in the clusters [10,14]. In addition, the plastic flow is generally inhibited in the center of highly concentrated clusters, due to the high level of hydrostatic stress [15]. Thus, particle clusters are preferred nucleation sites for cracks. The cracks emanate from locations where small matrix regions are surrounded by particles, leading to strain localization, early particle/matrix decohesion, and particle fracture. On the other hand, the inhomogeneity of the stress distribution in clustered MMCs has a strong influence on the global mechanical properties. It has been shown that the particle clustering decreases the flow stress of MMCs, compared to a composite with a homogeneous particle distribution [12]. A strong decrease in the global fracture toughness with increasing the content of clustering has been reported in an Al–SiC MMC [16]. Hence, the spatial distribution of reinforcement in MMCs is one of the most important microstructural features.

Processes like mechanical alloying or rapid solidification have been tested to overcome the agglomeration of reinforcements; however, these methods are accompanied by contamination, porosity, and poor economical efficiency [17–19]. Additionally, conventional secondary deformation processing methods like rolling and/or extrusion have been used to improve the homogeneity of the particle distribution [9,13]. Nonetheless, this is difficult or impossible in the case of fine particles, since very high strains would be required [13]. It has been identified that severe plastic deformation (SPD) can be successfully applied to improve the homogeneity of the particle distribution in MMCs. Typically, Sabirov et al. [20] have studied the homogenization of Al–SiC and Al–Al_2O_3 powder metallurgy (PM) MMCs via high-pressure torsion. The homogeneity evolution of a strongly clustered particle distribution in PM Al–Al_2O_3 MMCs during equal channel angular pressing has been also focused [21]. Accumulative roll bonding (ARB) has several advantages over other SPD processes, including (1) high load capacity forming facilities and expensive dies are not needed, (2) productivity rate is high, and (3) the content of material to be produced is not limited. The

This is the accepted manuscript (postprint) of the following article:
A. Yazdani, E. Salahinejad, *Evolution of reinforcement distribution in Al–B_4C composites during accumulative roll bonding*, Materials & Design, 32 (2011) 3137-3142.
https://doi.org/10.1016/j.matdes.2011.02.063

ARB process consists of multiple cycles of rolling, cutting, stacking and solid-state deformation bonding. In this paper, the distribution evolution of B_4C reinforcing particulates in an Al matrix composite during ARB is investigated by microscopic and bulk hardness evaluations.

2. Experimental procedures

2.1. Sample preparation

1050-Aluminum alloy strips of 250 mm long, 90 mm wide, and 0.4 mm thick and B_4C powders with an average size of 3 μm were used as the raw materials. To produce Al–10 vol.% B_4C composites, the eight Al strips, which were degreased in acetone and scratch brushed (surface preparation), were stacked over each other, while 1.1 vol.% B_4C powders were dispersed between each pair of the strips. The strips were roll-bonded with a draft percentage of 66% reduction, according to Ref. [22], at room temperature. In this paper, this processing part is named as Step 1. The roll-bonded strip was cut into three strips and annealed at 623 K for 1 h. After the surface preparation, the three strips were stacked, 1.1 vol.% B_4C powders were dispersed between them, and roll-bonded again (Step 2).

The next stage of the production sequence was the ARB process. The roll-bonded strip obtained from Step 2 was cut into two strips and annealed. After the surface preparation, the two strips were stacked over each other (without dispersing the B_4C particles) and roll-bonded with a draft percentage of 50% reduction. This procedure was defined as one ARB cycle and repeated to seven times without annealing between each cycle. The rolling processes were carried out with the rolling speed of 15 rpm and the roll diameter of 150 mm, without any lubrication.

This is the accepted manuscript (postprint) of the following article:
A. Yazdani, E. Salahinejad, *Evolution of reinforcement distribution in Al–B$_4$C composites during accumulative roll bonding*, Materials & Design, 32 (2011) 3137-3142.
https://doi.org/10.1016/j.matdes.2011.02.063

2.2. Materials characterization

The crystallite size of the Al matrix was determined by X-ray diffraction (XRD, Philips Analytical PC-APD with a Cu ka radiation) peak profile analysis. Indeed, XRD peaks are broadened when crystallites are small or the material contains lattice defects. Size and strain broadening can be separated by the Williamson-Hall procedure which is based on the full widths at half maximum (FWHM) or the integral breadths, providing the apparent size parameters of coherently scattering domains (crystallites) and the values of the mean square strain, as follows:

$$B\cos\theta = \frac{k\lambda}{D} + 2\varepsilon\sin\theta$$

where B is FWHM of a diffraction peak, k is a constant, k is the X-ray wavelength, h is the Bragg angle, D is the crystallite size, and e is the lattice strain. In this method, B cos h is plotted vs. sin h and the intercept of the linear extrapolation yields the crystallite size. The Gaussian assumption was used to separate the intrinsic and instrumental broadenings, because of the fact that the environment in the diffractometer was not ideal.

An optical microscope (OM) was used to observe the dispersion of the B$_4$C particles in the rolling direction (RD)–normal direction (ND) plane of the composites. The optical micrographs were analyzed by the radial distribution function to quantify the reinforcement distribution. Karnezis et al. [23] pointed out that the radial distribution function is an effective method to detect pronounced changes in MMCs. In the radial distribution function, a circular disc of radius r is centered on the gravity center of a particle and the function H(r) is determined as:

$$H(r) = \frac{N_{ra}}{N_a}$$

where N_{ra} is the mean number of the particles per unit area in a disc of radius r and N_a is the mean number of the particles per unit area over the whole sample. Compared with a Poisson pattern that reflects a homogeneous particle distribution, the function H(r) for a random distribution of particles has a constant value of 1; on the contrary, the function H(r) for a strongly clustered distribution displays a pronounced peak before settling rapidly to 1. The degree of clustering was also estimated by the deviation of the experimental H(r) curves from H(r) = 1 via the area A_H. The function H(r) and the area A_H were described by [23]:

$$H(r) = ae^{-br} + c$$

$$A_H = \int_{r=10\ \mu m}^{r=100\ \mu m} [H(r) - 1]dr$$

where a, b, and c are constants. To determine the radial distribution function, a range of radii from r = 10 µm to r = 100 µm was considered.

Vickers bulk hardness tests, using a load of 150 g for 15 s, were performed on the RD–ND plane of the samples. The average value of 10 separated measurements taken at randomly selected points was reported and the related standard deviations were calculated.

3. Results and discussion

The XRD pattern and Williamson-Hall plot of the composite processed by seven ARB cycles are shown in Fig. 1. From the intercept of the Williamson-Hall plot, the area weighted mean crystallite size was calculated to be 114 nm, with the R-squared value of 0.957. That is, the ARB process to seventh cycle has successfully developed a nanostructured Al–B_4C MMC,

This is the accepted manuscript (postprint) of the following article:
A. Yazdani, E. Salahinejad, *Evolution of reinforcement distribution in Al–B_4C composites during accumulative roll bonding*, Materials & Design, 32 (2011) 3137-3142.
https://doi.org/10.1016/j.matdes.2011.02.063

which is in good agreement with Refs. [24,25]. Structural refinement can be explained in terms of grain subdivision at a submicron scale, where initial coarse grains are subdivided by deformation-induced high-angle grain boundaries [26–28].

It would be worth mentioning that, particularly in plastically deformed materials, the crystallite sizes measured by the XRD peak profile analysis correspond to dislocation cells or subgrain sizes, where the variations of orientations are smaller than a few degrees. It is due to the fact that dislocation cell walls, arranged either in small-angle grain boundaries or dipolar-wall configurations, break down the coherency of the X-ray scattering [29]. It should be considered that crystallites determined from the X-ray line broadening are smaller than the related grains observed by transmission electron microscope (TEM), due to the subdivision of the grains into substructures [30]. From TEM observations, it has been reported that a pancake shaped or elongated lamellar ultrafine structure is formed in Al–7.5 vol.% B_4C processed by eight ARB cycles, in which the average lamellar and transverse boundary spacings were about 186 and 560 nm, respectively [31]. Note that lamellar boundaries are almost parallel to RD and short transverse boundaries interconnect the lamellar boundaries. The detailed correlation between grain or crystallite sizes obtained by TEM and X-ray line broadening has been focused in Ref. [29].

This is the accepted manuscript (postprint) of the following article:
A. Yazdani, E. Salahinejad, *Evolution of reinforcement distribution in Al–B_4C composites during accumulative roll bonding*, Materials & Design, 32 (2011) 3137-3142.
https://doi.org/10.1016/j.matdes.2011.02.063

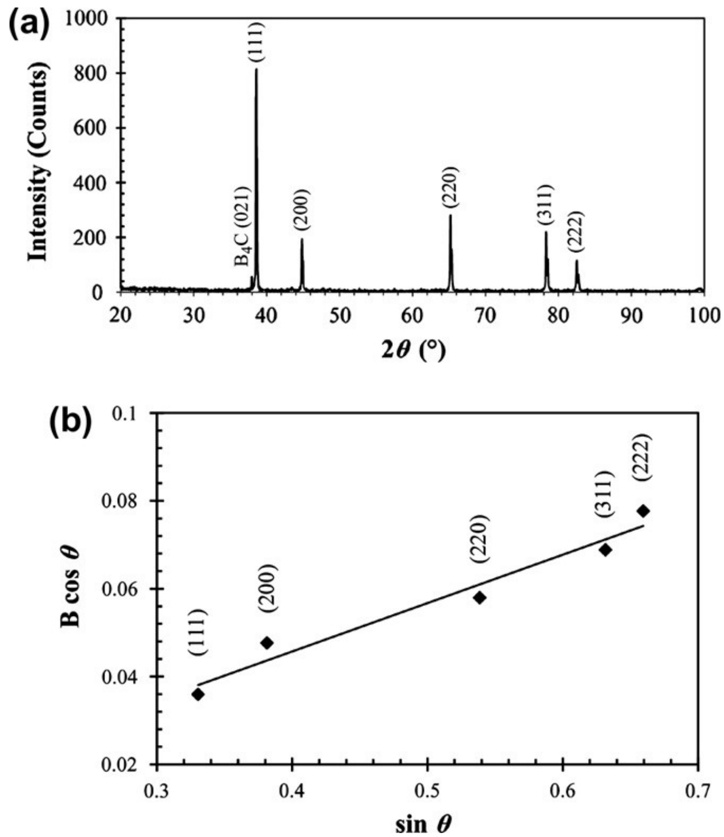

Fig. 1. XRD pattern (a) and Williamson-Hall plot (b) of the composite processed by seven ARB cycles.

Fig. 2 depicts the optical micrograph of the specimen after Step 1 taken from the RD–ND plane. Note that this sample includes 7.7 vol.% B_4C, and the remainder of the particles was imported in Step 2 to obtain the Al–10 vol.% B_4C composite. The separated layers of both the constituents (Fig. 2a), significant particle clusters (Fig. 2b), and large particle-free zones are well recognizable, which is an undesirable structure from the reinforcement distribution viewpoint. Moreover, it can be seen that the level of dense particle clusters elongated in RD prevail over that of diffuse clusters situated around the dense clusters. Dense particle clusters are denominated as particle agglomerations where no matrix material is present between the

This is the accepted manuscript (postprint) of the following article:
A. Yazdani, E. Salahinejad, *Evolution of reinforcement distribution in Al–B4C composites during accumulative roll bonding*, Materials & Design, 32 (2011) 3137-3142.
https://doi.org/10.1016/j.matdes.2011.02.063

particles, while particle clusters with some amount of the matrix material between the particles are denominated as diffuse clusters.

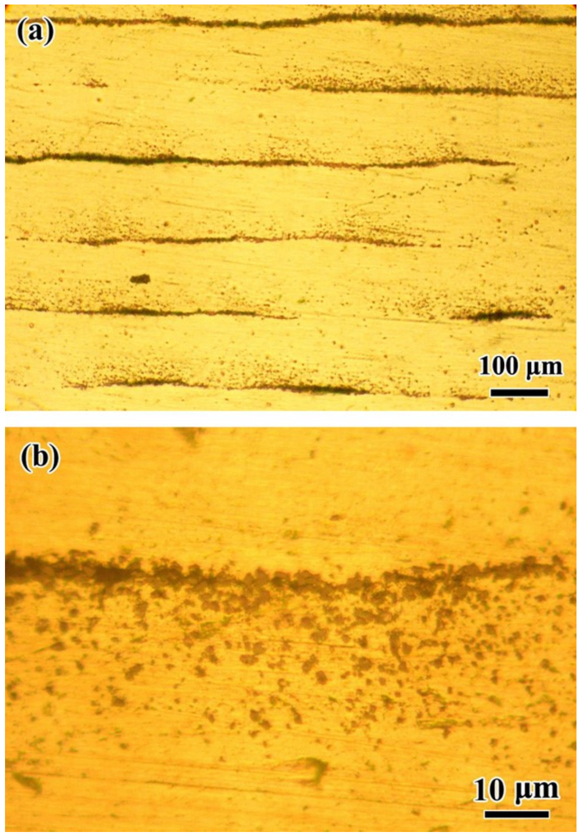

Fig. 2. Optical micrograph of the RD–ND plane of the specimen after Step 1 in two magnifications.

The typical optical micrographs of the Al–10 vol.% B_4C composites processed by the ARB process taken from the RD–ND plane are signified in Fig. 3. In the composite fabricated by one ARB cycle, dense and diffuse B_4C particle clusters are still observed (Fig 3a). Compared to Fig. 2, the elongated dense clusters have dissociated into several smaller dense particle clusters. Therefore, the number of particle clusters in the investigated area increases. It is noticeable that the further increase in ARB cycles leads to a decrease in the level of observed

This is the accepted manuscript (postprint) of the following article:
A. Yazdani, E. Salahinejad, *Evolution of reinforcement distribution in Al–B₄C composites during accumulative roll bonding*, Materials & Design, 32 (2011) 3137-3142.
https://doi.org/10.1016/j.matdes.2011.02.063

particle clusters (declustering) and the shrinkage of particle-free zones (Fig. 3b–d), suggesting a gradual improvement in the particle distribution. No particle-free zones and particle clusters are nearly observed in the specimen processed by seven ARB cycles. That is, the particle distribution appears to be pleasingly homogeneous in this MMC specimen. It is also noted that detailed microstructural investigations reflect that no particle fracture occurs during the ARB process.

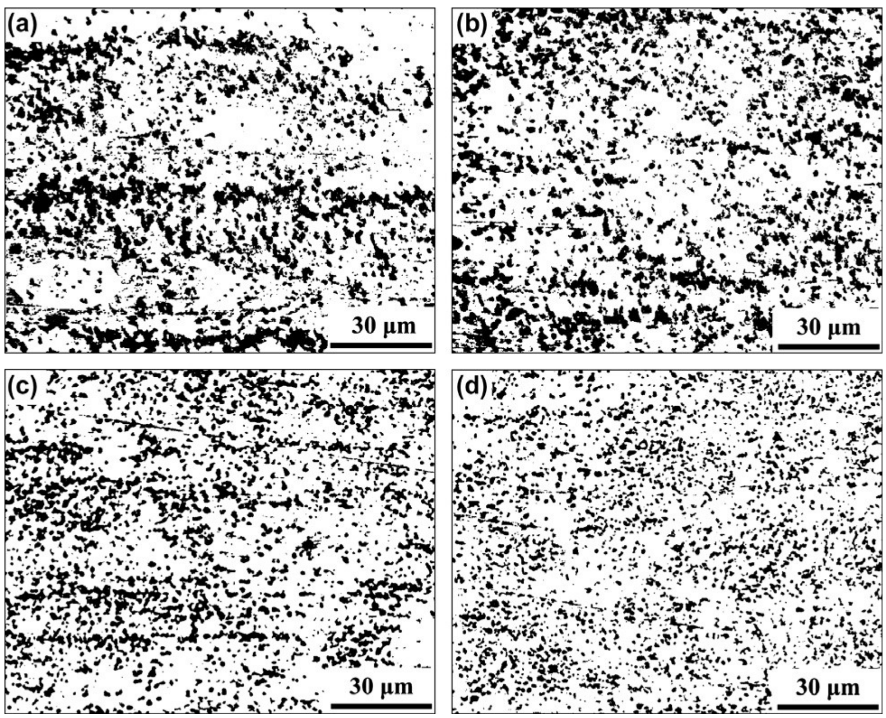

Fig. 3. Typical optical micrograph of the RD–ND plane of the Al–B_4C composites processed by the ARB process to one (a), three (b), five (c), and seven (d) cycles.

The variation in the radial distribution function H(r) was also employed to quantify the B_4C distribution in the produced MMCs. A random distribution of the B_4C particles yields H(r) = 1 for any disc radius r. On the other hand, the H(r) curves for clustered B_4C distributions would show a sharp peak at small r values, rapidly dropping to a plateau of approximately 1

This is the accepted manuscript (postprint) of the following article:
A. Yazdani, E. Salahinejad, *Evolution of reinforcement distribution in Al–B₄C composites during accumulative roll bonding*, Materials & Design, 32 (2011) 3137-3142.
https://doi.org/10.1016/j.matdes.2011.02.063

at larger r values. Fig. 4 reveals the radial distribution function H(r) plots, based on Eq. (2) in the range r = 10–100 µm, for the Al–B_4C composites produced by the ARB process. Note that this analysis was performed on the optical micrograph of the RD–ND plane of the composites. Typically, for the composite processed by one ARB cycle, the H(r) values are decreased from 5.3 to 1.29, and for that processed by seven ARB cycles, those are decreased from 4.1 to 1.1 when the disc radius r increases from 10 µm to 100 µm. By increasing the number of ARB cycles, a decrease in the height of the initial peak at low r values in the H(r) plots is observed, implying an improvement in the particle distribution uniformity.

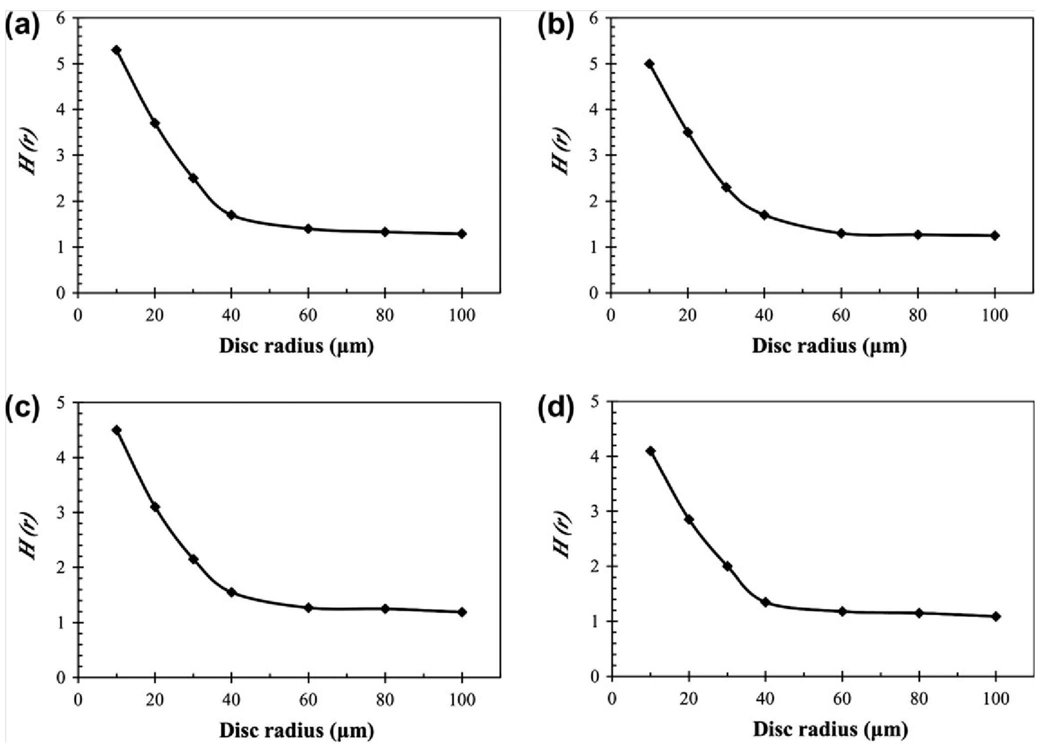

Fig. 4. Typical radial distribution function H(r) plots for the Al–B_4C composites produced by the ARB process to one (a), three (b), five (c), and seven (d) cycles.

The degree of clustering (A_H) that is estimated by Eqs. (3) and (4) is presented in Fig. 5. The A_H values are decreased from 115 µm to 71 µm for the composites processed by one to seven

This is the accepted manuscript (postprint) of the following article:
A. Yazdani, E. Salahinejad, *Evolution of reinforcement distribution in Al–B_4C composites during accumulative roll bonding*, Materials & Design, 32 (2011) 3137-3142.
https://doi.org/10.1016/j.matdes.2011.02.063

ARB cycles. Considering that larger A_H values are indicative of increased particle inhomogeneity, it is inferred from this assessment that by increasing the number of ARB cycles, an improvement in the microstructure uniformity is obtained, which is well compatible with H(r) and the observed microstructures.

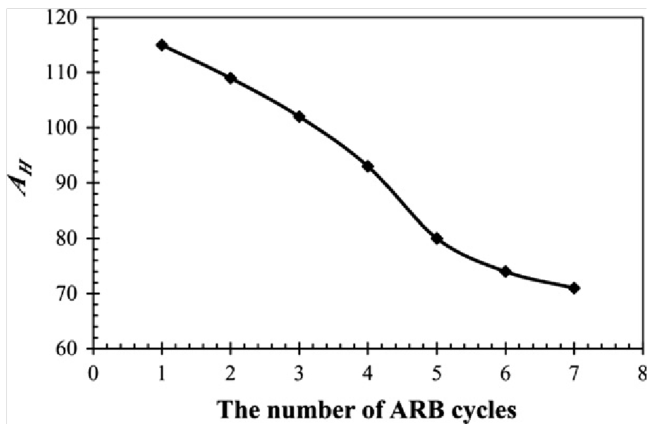

Fig. 5. Degree of clustering (A_H) of the Al–B_4C MMCs produced by the ARB process.

The hardness values of the Al–B_4C composites as a function of ARB cycles are illustrated in Fig. 6. The curve indicates an immediate increase in hardness at the initial cycles, followed by a minor additional increase to the seventh cycle. After seven ARB cycles, the hardness of the composite reached 82 HV. The rapid increase in the hardness behavior at the initial cycles is owing to strain hardening, i.e. an increase in the density of dislocations and interaction between them, which is saturated at large strains [31]. In the initial cycles, the sample has a layered structure, in which the B_4C powder layers keep apart the Al layers. By increasing cycles, the distribution of the B_4C reinforcing particles in the matrix is improved, thereby increasing the composite hardness. Furthermore, the decrease of porosities in the Al matrix by increasing cycles is another source of the increased hardness trend. It can be also seen that the standard deviation of the measurements is decreased by increasing the number of cycles.

https://doi.org/10.1016/j.matdes.2011.02.063

It is another evidence for this fact that by increasing cycles, the uniformity is improved. In the case of the inhomogeneity, a number of indents can be applied on particle-free zones showing low hardness values and a number of indents can be applied on particle clusters depicting high hardness values; therefore, the standard deviation of the ten random indentations present a large value. In contrast, in the case of the structure uniformity, the contribution of the matrix and reinforcement to the hardness value is almost the same in all locations of the investigated area, showing a low standard deviation.

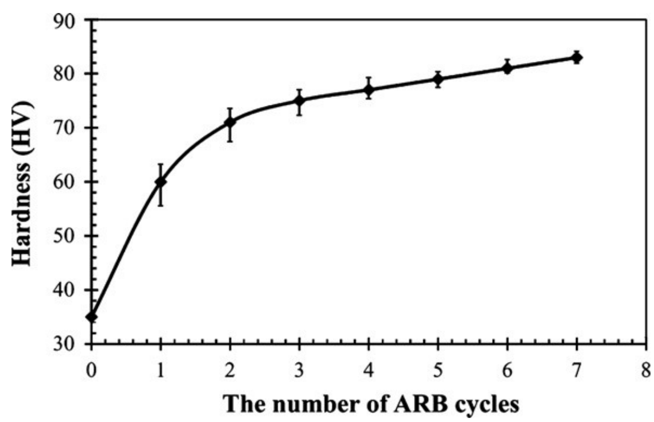

Fig. 6. Hardness values of the Al–B_4C composites produced by the ARB process.

The microscopic investigations quantified by the radial distribution function analysis (Figs. 3–5), as well as the observed decrease in the standard deviation of the hardness values (Fig. 6) confirmed that the microstructure uniformity is improved by increasing the number of ARB cycles. It has been found that during the high-pressure torsion of MMCs, the declustering process of dense particle clusters occurs via particle debonding from the cluster surface and moving into the particle-free matrix (cluster erosion); in contrast, the deformation of diffuse particle clusters is mainly responsible for homogenization [20]. In the present study, the evolution of the B_4C reinforcement distribution during ARB is regarded from three viewpoints:

i. The increase in the number of the Al and B_4C layers. Clearly, by progression of ARB, the number of the Al and B_4C layers is increased. As noted in the experimental section, after Step 1 there are the seven layers of the B_4C powder particles and the eight layers of the Al matrix. The number of the layers of the B_4C powder particles and the Al matrix approach 23 (23 = [7 × 3] + 2) and 24 (24 = 8 × 3) respectively after Step 2. The number of the layers of the B_4C powder particles and the Al matrix after the ARB process to n cycles is 23×2^n and 24×2^n, respectively. For instance, the composite fabricated by seven ARB cycles is composed of the 2944 layers of the B_4C particles and the 3072 layers of the Al matrix. Undoubtedly, the increase in the number of the Al and B_4C layers dictates an improvement in the particle distribution in ND.

ii. The metal extrusion through particle clusters. In accordance with the film theory, during rolling, the two opposing brittle surface oxide layers produced by surface preparation fragment to expose the underlying metals which are extruded under the normal roll pressure through cracks in the oxide layers from both sides of the interfaces [32,33]. In the same way, in the presence of the B_4C particles between the Al strips, the matrix material is extruded and flows through particle clusters. As a result, dense particle clusters are converted to diffuse clusters, and the distance between the particles constituting the clusters is enhanced, suggesting the dissociation of the clusters and the improvement of the reinforcement distribution.

iii. The sheet elongation due to rolling. During the rolling process, an amount of sheet elongation along RD, which is a function of the reduction level, occurs. This fundamental fact can explain the evolution of the particle distribution in the RD–TD plane. The

This is the accepted manuscript (postprint) of the following article:
A. Yazdani, E. Salahinejad, *Evolution of reinforcement distribution in Al–B_4C composites during accumulative roll bonding*, Materials & Design, 32 (2011) 3137-3142.
https://doi.org/10.1016/j.matdes.2011.02.063

deformation and elongation of particle clusters of MMCs in RD during standard secondary processing like rolling have been previously pointed out [3,13]. Particle clusters are elongated in RD due to the sheet elongation, promoting the cluster expansion and the transition of dense-to-diffuse clusters, as accompanied by the matrix infusion between the particles. It means the increase of the distance of clusters' particles, the dissociation of clusters, the shrinkage of particle-free zones, and finally an improvement in the microstructure homogeneity.

4. Conclusions

The outcome of this study can be summarized as follows:

- The ARB process to seven cycles resulted in nanocrystallization in the matrix of the Al–B_4C composite.
- By progression of ARB from one to seven cycles, the overall hardness was increased from 60 HV to 82 HV.
- The microscopic studies accompanied by the radial distribution function analysis and the hardness evaluations suggested an improvement in the reinforcement distribution by increasing ARB cycles.
- The improved uniformity was explained in terms of the increase in the number of the Al and B_4C layers, the metal extrusion through particle clusters, and the sheet elongation due to rolling by progression of ARB.

This is the accepted manuscript (postprint) of the following article:
A. Yazdani, E. Salahinejad, *Evolution of reinforcement distribution in Al–B_4C composites during accumulative roll bonding*, Materials & Design, 32 (2011) 3137-3142.
https://doi.org/10.1016/j.matdes.2011.02.063

Acknowledgment

The authors would like to thank the laboratory technicians of Shiraz University (Department of materials science and engineering) for their technical assistance in conducting this project.

References

[1] Kaczmar JW, Pietrzak K, Wlosinski W. The production and application of metal matrix composite materials. J Mater Process Technol 2000; 106: 58–67.

[2] Wang HY, Jiang QC, Wang Y, Ma BX, Zhao F. Fabrication of TiB_2 particulate reinforced magnesium matrix composites by powder metallurgy. Mater Lett 2004; 58: 3509–13.

[3] Torralba JM, da Costa CE, Velasco F. P/M aluminum matrix composites: an overview. J Mater Process Technol 2003; 133: 203–6.

[4] Liu CH. Structure and properties of boron carbide with aluminum incorporation. Mater Sci Eng B 2000; 72: 23–6.

[5] Fogagnolo JB, Ruiz-Navas EM, Robert MH, Torralba JM. The effects of mechanical alloying on the compressibility of aluminium matrix composite powder. Mater Sci Eng A 2003; 355: 50–5.

[6] Shorowordi KM, Haseeb A, Celis JP. Tribo-surface characteristics of Al–B_4C and Al–SiC composites worn under different contact pressures. Wear 2006; 261: 634–641.

[7] Chapman TR, Niesz DE, Fox RT, Fawcett T. Wear-resistant aluminum–boron–carbide cermets for automotive brake applications. Wear 1999; 236: 81–8.

[8] Bermudez M, Carrion FJ, Iglesias P, Martinez-Nicolas G, Herrera EJ, Rodriguez JA. Influence of milling conditions on the wear resistance of mechanically alloyed aluminium. Wear 2005; 258: 906–14.

[9] Clyne TV, Withers PJ. An Introduction to Metal Matrix Composites. Cambridge, United Kingdom: Cambridge University Press; 1993.

[10] Lloyd DJ. Aspects of fracture in particulate reinforced metal matrix composites. Acta Metall Mater 1991; 42: 59–71.

[11] Wang Z, Chen TK, Lloyd DJ. Stress distribution in particulate-reinforced metalmatrix composites subjected to external load. Metall Trans A 1993; 24: 197–207.

[12] Christman T, Needleman A, Suresh S. An experimental and numerical study of deformation in metal-ceramic composites. Acta Metall 1989; 37: 3029–50.

[13] Tan MJ, Zhang X. Powder metal matrix composites: selection and processing. Mater Sci Eng A 1998; 244: 80–5.

[14] Wang Z, Zhang RJ. Mechanical behavior of cast particulate SiC/Al (A356) metal matrix composites. Metall Trans A 1991; 22: 1585–93.

[15] Prangnell PB, Barnes SJ, Roberts SM, Withers PJ. The effect of particle distribution on damage formation in particulate reinforced metal matrix composites deformed in compression. Mater Sci Eng A 1996; 220: 41–56.

[16] Tao S, Townely N, Boyd JD. Effects of particulate spacing distribution on internal stress and damage in MMCs. Microstruct Sci 1994; 22: 249–59.

[17] Upadhyaya A, Upadhyaya GS. Sintering of copper–alumina composites through blending and mechanical alloying powder metallurgy routes. Mater Des 1995; 16: 41–5.

[18] Ferkel H. Properties of copper reinforced by laser-generated Al_2O_3– nanoparticles. Nanostruct Mater 1999; 11: 595–602.

[19] Ying DY, Zhang DL. Processing of Cu–Al2O3 metal matrix nanocomposite materials by using high energy ball milling. Mater Sci Eng A 2000; 286:
152–6.

[20] Sabirov I, Kolednik O, Pippan R. Homogenization of metal matrix composites by high-pressure torsion. Metall Mater Trans A 2005; 36: 2861–70.

[21] Sabirov I, Kolednik O, Valiev RZ, Pippan R. Equal channel angular pressing of metal matrix composites: effect on particle distribution and fracture toughness. Acta Mater 2005; 53: 4919–30.

[22] Alizadeh M, Paydar MH. Study on the effect of presence of TiH_2 particles on the roll bonding behavior of aluminum alloy strips. Mater Des 2009; 30: 82–6.

[23] Karnezis PA, Durrant G, Cantor B. Characterization of reinforcement distribution in cast Al–Alloy/SiCp composites. Mater Charact 1998; 40: 97–109.

[24] Saito Y, Tsuji N, Utsunomiya H, Sakai T, Hong RG. Ultra-fine grained bulk aluminum produced by accumulative roll-bonding (ARB) process. Scripta Mater 1998; 39: 1221–7.

[25] Tsuji N, Iwata T, Sato M, Fujimoto S, Minamino Y. Aging behavior of ultrafine grained Al–2 wt%Cu alloy severely deformed by accumulative roll bonding. Sci Technol Adv Mater 2004; 5: 173–80.

[26] Utsunomiya H, Tanda K, Saito Y, Sakai T, Tsuji N. Effects of lubrication on Accumulative Roll-Bonding (ARB) of aluminum. J Jpn Soc Technol Plas 1999; 40: 1187–91.

[27] Lee SH, Saito Y, Tsuji N, Utsunomiya H, Sakai T. Role of shear strain in ultragrain refinement by accumulative roll-bonding (ARB) process. Scripta Mater 2002; 46: 281–5.

[28] Liu Q, Hansen N. Macroscopic and microscopic subdivision of a cold-rolled aluminium single crystal of cubic orientation. Proc R Soc London A 1998; 454: 2555–91.

[29] Ungar T, Tichy G, Gubicza J, Hellmig R. Correlation between subgrains and coherently scattering domains. Powder Diffr 2005; 20: 366–75.

[30] Ungar T, Gubicza J. Grain size, size-distribution and dislocation structure from diffraction peak profile analysis. In: Zhu YT, Langdon TG, Mishra RS, Semiatin SL, Saran MJ, Lowe TC, editors. Ultrafine grained materials II. Pennsylvania: TMS Publication; 2002. p. 595–604.

[31] Alizadeh M. Comparison of nanostructured Al/B_4C composite produced by ARB and Al/B_4C composite produced by RRB process. Mater Sci Eng A
2010; 528: 578–82.

[32] Vaidyanath LR, Nicholas MG, Milner DR. Pressure welding by rolling. Br Weld J 1959; 6: 13–28.

[33] Mohamed HA, Washburn J. Mechanism of solid state pressure welding. Weld J 1975; 30: 302–10.